Neutron-powder-diffraction study of the nuclear and magnetic structures of $YBa_2Fe_3O_8$ at room temperature

Q. Huang
Reactor Radiation Division, National Institute of Standards and Technology, Gaithersburg, Maryland 20899

P. Karen
Department of Chemistry, University of Oslo, Blindern, N-0315 Oslo 3, Norway

V. L. Karen
Reactor Radiation Division, National Institute of Standards and Technology, Gaithersburg, Maryland 20899

A. Kjekshus
Department of Chemistry, University of Oslo, Blindern, N-0315 Oslo 3, Norway

J. W. Lynn
Reactor Radiation Division, National Institute of Standards and Technology, Gaithersburg, Maryland 20899 and Center for Superconductivity Research, Department of Physics, University of Maryland, College Park, Maryland 20742

A. D. Mighell
Reactor Radiation Division, National Institute of Standards and Technology, Gaithersburg, Maryland 20899

N. Rosov
Reactor Radiation Division, National Institute of Standards and Technology, Gaithersburg, Maryland 20899 and Center for Superconductivity Research, Department of Physics, University of Maryland, College Park, Maryland 20742

A. Santoro
Reactor Radiation Division, National Institute of Standards and Technology, Gaithersburg, Maryland 20899
(Received 19 August 1991)

The nuclear and magnetic structures of $YBa_2Fe_3O_8$ have been investigated by powder neutron diffraction at room temperature. The nuclear structure of the compound has the symmetry of space group $P4/mmm$ and lattice parameters $a=3.9170(1)$ and $c=11.8252(4)$ Å. The configuration of the atoms in the unit cell is very similar to that of the superconductor $YBa_2Cu_3O_7$, with the exception that the iron ions corresponding to the Cu-chain ions have octahedral coordination, rather than square planar; the octahedra thus are arranged in layers rather than in chains. This significant difference is a consequence of the fact that all possible oxygen sites in these layers are fully occupied, resulting in an oxygen content of eight rather than seven atoms per formula unit. A second consequence of the full occupancy of the oxygen sites is that the Ba ions have a twelvefold cuboctahedral coordination in the iron compound, rather than tenfold. The magnetic structure is based on a unit cell related to that of the nuclear structure by an axis transformation of matrix $(1\bar{1}0/110/002)$. The magnetic origin of the extra intensities and the basic spin configuration were determined by polarized-neutron-diffraction measurements. The iron moments are coupled antiferromagnetically within each FeO_2 layer, as well as along the c axis. The magnetic moments of all the iron ions are the same with a value of $3.49(2)\mu_B$. This configuration results in the magnetic symmetry $I_c mm'm$.

INTRODUCTION

The substitution of copper by other metal species in the structure of $YBa_2Cu_3O_{6+x}$ has been used extensively to investigate the correlation between the modifications induced in the structure by the substituting cations and the changes in the superconducting properties. The first studies in this direction involved the partial replacement of either the chain copper atoms [indicated as Cu(1) in what follows],[1-5] or the plane copper atoms [indicated as Cu(2)].[6,7] From these experiments it was found that the introduction of dopants in the structure decreases the value of T_c and that this change is very drastic when the ions Cu(2) are replaced by even a small number of other ions such as Zn and Ni. These results were taken as evidence that the two-dimensional $Cu(2)O_2$ layers play a more important role than the chain layers in the superconducting process.

Partial replacement of the Cu(1) atoms by other cations with the same or a different type of coordination invariably introduces disorder in the configuration of the oxy-

 ©1992 The American Physical Society

gen atoms located in the basal plane of the structure [plane of the Cu(1) atoms]. Complete substitution of Cu(1), on the other hand, may circumvent this problem and help to clarify both the distribution of the oxygen atoms on the basal plane of the original 1:2:3 compound and the mechanism by which they diffuse. Successful attempts to substitute all the Cu(1) atoms in systems such as $LaBa_2(MCu_2)O_8$ (M=Ta, Nb) (Refs. 8–10) and $YSr_2(NCu_2)O_7$ (N=Ga, Co, Al), (Refs. 11–13) have been reported recently. These derivatives have been characterized both chemically and structurally. In the first system, the copper in the square chains of the parent $YBa_2Cu_3O_7$ is replaced by Ta or Nb and this requires the presence of extra oxygen, giving the composition of eight atoms per formula unit in order to satisfy the octahedral coordination of these cations. In the second system, Ga, Co, and Al have tetrahedral coordination. This does not result in a compositional change, but causes a drastic rearrangement of the oxygen atoms located in the chain layer.

Full substitution of Cu(1) and Cu(2) by Co has been accomplished with simultaneous partial replacement of Ba by K.[14] The resulting compound, with a claimed composition $Y(K_{0.5}Ba_{1.5})Co_3O_8$, was characterized by x-ray powder diffraction and was found to have the basic $YBa_2Cu_3O_{6+x}$ structure with Co(1) octahedrally coordinated and Co(2) in a fivefold pyramidal coordination. To our knowledge, no other fully substituted compounds have been prepared and characterized so far. This is surprising since information about the precise structure of copper-free compounds of this type is important for understanding why copper, of all the transition metals, seems to be necessary for superconductivity to occur.

A phase having the same metal stoichiometry of $YBa_2Cu_3O_{6+x}$, but with copper entirely replaced by iron, was identified during an ongoing study of the substitution of copper with other transition metals.[15] Structural studies of this phase, $YBa_2Fe_3O_8$, were carried out at room temperature by neutron powder diffraction, and the results of this work are reported in this paper.

EXPERIMENTAL RESULTS

The 30-g sample of $YBa_2Fe_3O_8$ used in the present study was prepared from liquid-mixed-citrate precursors. Reagent-grade starting materials (Fe powder, Y_2O_3, and $BaCO_3$) were dissolved in citric acid and the resulting clear citrate gel was dehydrated, milled, and repeatedly fired in a stream of purified carbon- and hydrogen-free oxygen with intermittent rehomogenizations. Pellets of the sample, placed on a layer of the master sample in a corundum boat, were subjected to five firing cycles, each of 300-h duration, at temperatures from 950 to 1000 °C. The last cycle was concluded with a 30-h oxidation at 340 °C in oxygen. The sample was checked for the presence of carbonate by determining the amount of CO_2 released after heating the sample in flowing O_2 at 1100 °C. No carbon was detected within experimental error (0.03 wt. %). The oxygen content could then be determined gravimetrically by reduction in ultrapure hydrogen ($\geq$99.99%) at 1000 °C. The completeness of this reduction was checked by x-ray diffraction. The analysis gave a composition corresponding to the formula $YBa_2Fe_3O_{8.00(3)}$.

Neutron-powder-diffraction measurements were made at room temperature using the high-resolution five-counter diffractometer at the Reactor of the National Institute of Standards and Technology, with the experimental conditions given in Table I. All refinements were carried out using the Rietveld method,[16] adapted to the multicounter diffractometer and modified to include the background parameters.[17] The peak shape was described by a Pearson function and the neutron-scattering amplitudes used in the calculations were b(Y)=0.775, b(Ba)=0.525, b(Fe)=0.954, and b(O)=0.581$\times 10^{-12}$ cm.

The first refinement was made using a model with initial parameters similar to those obtained for the structure of $YBa_2Cu_3O_7$. The assumed symmetry of the model, however, was that of space group $P4/mmm$, rather than $Pmmm$, with the position at ($\frac{1}{2}$,0,0) on the basal plane fully occupied by oxygen atoms. This configuration corresponds to a composition O_8, in agreement with the results of the chemical analysis. This first set of calculations resulted in unacceptably high R factors (R_N=9.27, R_P=9.70, R_W=16.34 with an expected value R_E=5.48). More significantly, some strong observed intensities, mainly present in the low-angle region of 2θ, and in particular a strong reflection at $2\theta \simeq 20°$, were not

TABLE I. Collection of intensity data.

Monochromatic beam:	Reflection 220 of a Cu monochromator
Wavelength:	1.545(1) Å
Horizontal divergences:	10′, 20′, 10′ of arc for the in-pile, monochromatic beam, and diffracted beam collimators, respectively
Sample container:	Vanadium can of about 10 mm diameter in an aluminum holder
2θ angular range:	5°–120°, steps: 0.05°

Measurements made at room temperature

accounted for by the adopted model. These extra reflections could be indexed in terms of a larger unit cell of parameters $a=b=a_0\sqrt{2}$ and $c=2c_0$, where a_0 and c_0 are the lattice parameters corresponding to the cell of the 1:2:3-type structure. Attempts to shift the atoms in this cell from their idealized positions did not improve the agreement between observed and calculated intensities, as the atoms invariably tended to return to their original locations. Similarly, the possible presence of extra oxygen in the yttrium layer of the structure, or the existence of oxygen vacancies in the BaO and FeO_2 layers, or possible disordering between Ba and Y, had to be excluded since refinements of these defective models gave values of the occupancy factors equal, to within a few standard deviations, to those corresponding to the nondefective original structure. As mentioned previously, the unaccounted intensities occur at low values of θ. An attempt was therefore made to refine the initial 1:2:3 model using only the data with $60°<2\theta\leq 120°$. These calculations resulted in very satisfactory R factors ($R_N=4.83$, $R_P=5.94$, $R_W=8.33$, and $R_E=5.48$) and quite reasonable structural parameters, including temperature factors. This result shows that the extra intensities decrease rapidly with increasing diffraction angle and may be due to magnetic ordering of the iron ions. To verify that the observed scattering is indeed magnetic, two tests were carried out. In the first, a search was made for the strong reflection at $2\theta\simeq 20°$ using powder x-ray diffraction. No intensity was observed in the powder pattern at this angular position at the level of 0.1% of the 116 reflection, which is the strongest peak in the x-ray pattern (Fig. 1).

The second test involved the use of a primary beam of polarized neutrons and polarization analysis of the scattered neutrons. This experimental configuration can establish unambiguously if the additional peaks are magnetic in origin, and also may be used to separate the magnetic and nuclear scattering at angles where the magnetic and nuclear peaks overlap. The data were collected on the BT-2 triple-axis polarized beam spectrometer. Heusler alloy crystals in reflection geometry were employed as polarizing monochromator and analyzer. A wavelength of 2.3509 Å was chosen, with a pyrolytic graphite filter to suppress higher-order wavelengths. The collimation was 60'-60'-60'-open full width at half maximum (FWHM), and the instrumental flipping ratio was ≈ 11 under these conditions.

The polarization analysis technique as applied to this problem is in principle straightforward.[18] Nuclear coherent Bragg scattering never causes a reversal, or spin flip, of the neutron spin direction upon scattering. Thus the nuclear peaks will only be seen in the non-spin-flip [denoted by $(++)$] scattering geometry. The magnetic cross sections, on the other hand, depend on the relative orientation of the neutron polarization $\mathbf{P}$ and the reciprocal lattice vector transfer τ. In the configuration where $\mathbf{P}\perp\tau$ (vertical field), half the magnetic Bragg scattering involves a reversal of the neutron spin [denoted by the $(-+)$ configuration], and half does not. Thus, for a purely magnetic reflection the spin-flip $(-+)$ and non-spin-flip $(++)$ intensities should be equal in intensity. For the case where $\mathbf{P}\parallel\tau$ (horizontal field), all the magnetic scattering is spin-flip. Hence for a magnetic Bragg peak in the horizontal field configuration the spin-flip scattering should be twice as strong as for the $\mathbf{P}\perp\tau$ configuration, while ideally no non-spin-flip scattering will be observed.

Figure 2 shows the polarized beam results for two peaks at scattering angles 2θ (for this wavelength) of 30.26° and 35.02°. All the data were obtained at room temperature. The top section of the figure shows the data for the $\mathbf{P}\perp\tau$ configuration. The peak at 30.26° has the identical intensity for both spin-flip and non-spin-flip scattering, and we conclude that this scattering is purely magnetic in origin. These data alone unambiguously establish that this iron compound is magnetically long-range ordered. Indeed this peak coincides in position with the strongest magnetic reflection, (the 103 reflection; indexed as $\frac{1}{2}\frac{1}{2}\frac{3}{2}$ in Ref. 19) observed in the related

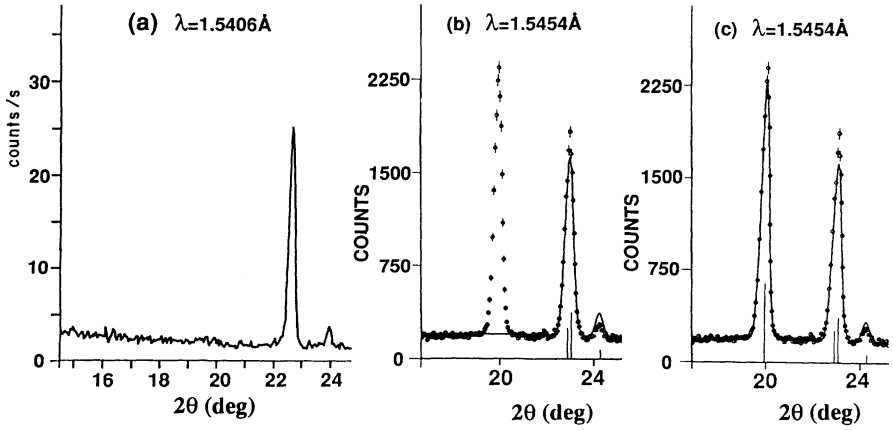

FIG. 1. Comparison of the x-ray and neutron powder patterns for 2θ between 17° and 25°. (a) X-ray pattern showing no diffracted intensity in the region of $2\theta\simeq 20°$. (b) Neutron pattern showing the measured intensities (open circles) and those calculated by taking into account the nuclear structure only (continuous line). The peak at $2\theta\simeq 20°$ is not accounted for by this model. (c) Fit of observed and calculated intensities when both the nuclear and magnetic structures are taken into consideration.

$YBa_2Cu_3O_{6+x}$ system,[19,20] when both the Cu planes and chains are ordered. Hence the same basic antiferromagnetic spin configuration may occur in this iron system, as discussed in detail below. The peak at 35.02°, on the other hand, has strong intensity for (+ +), while the intensity for (− +) is smaller by a factor of $\frac{1}{11}$. We conclude then that there is no spin-flip intensity other than that caused by the finite flipping ratio, and this peak is identified as a pure nuclear reflection.

The center section shows the same peaks for the $\mathbf{P}\|\tau$ configuration. The low-angle peak is now only observed in the spin-flip configuration, as expected for a magnetic reflection; the small peak observed in the (+ +) measurement is again due to the finite instrumental flipping ratio. The nuclear reflection, on the other hand, is only seen in the non-spin-flip configuration. The bottom section shows the subtraction of the $\mathbf{P}\perp\tau$ spin-flip scattering from the $\mathbf{P}\|\tau$ spin-flip scattering. In this subtraction procedure instrumental background, as well as all nuclear scattering cross sections, cancel, isolating the magnetic scattering. We see that there is magnetic intensity only for the low-angle position, while no intensity at the 35° peak position survives the subtraction.

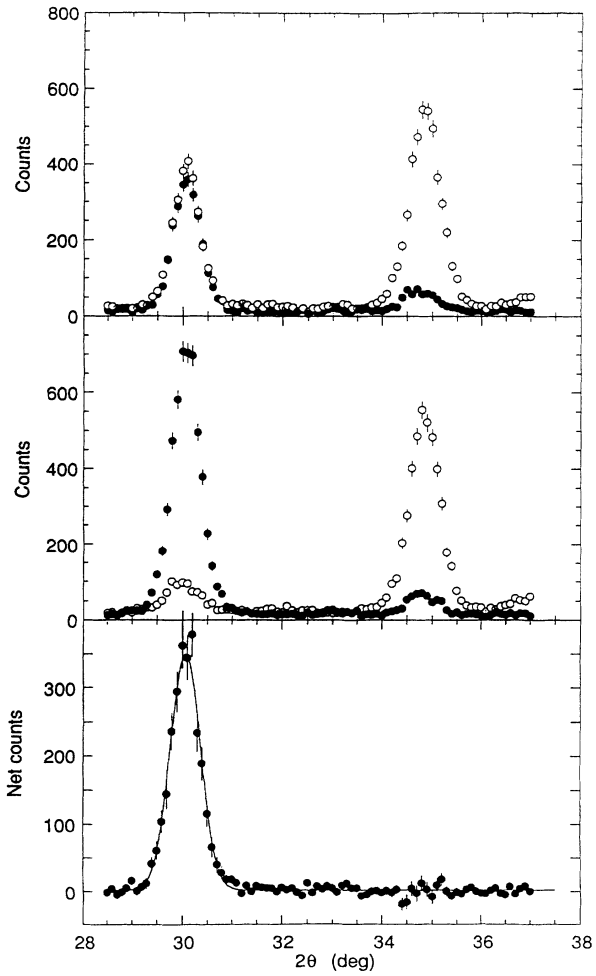

FIG. 2 Polarized neutron scattering observed over the 2θ angle range from 28.5° to 37°. The top portion of the figure is for the $\mathbf{P}\perp\tau$ configuration, where the open circles show the non-spin-flip scattering and the filled circles are the observed scattering in the spin-flip configuration. The low-angle peak has equal intensity for both cross sections, and thus is identified as a pure magnetic reflection, while the ratio of the (+ +) to (− +) scattering for the high-angle peak is 11, the instrumental flipping ratio. Hence this is a pure nuclear reflection. The center portion of the figure is for $\mathbf{P}\|\tau$, and the bottom portion is the subtraction of the $\mathbf{P}\perp\tau$ spin-flip data from the data for $\mathbf{P}\|\tau$. Note that in the subtraction procedure all background and nuclear cross sections cancel, isolating the magnetic scattering.

Figure 3 shows the same type of data for a peak at ~60°, which actually consists of several reflections; two magnetic reflections (the 109 and 123), a nuclear reflection from the sample (the 0 0 10 reflection), plus a nuclear reflection from the aluminum holder. Consequently this peak has intensity for both the (− +) and (+ +) configurations, as expected for a mixed reflection. The top portion of the figure shows the $\mathbf{P}\perp\tau$ data, the center is for $\mathbf{P}\|\tau$, and the bottom is the subtraction of the spin-flip $\mathbf{P}\perp\tau$ data from $\mathbf{P}\|\tau$, which reveals the magnetic component of the scattering. The fitted peak is the sum

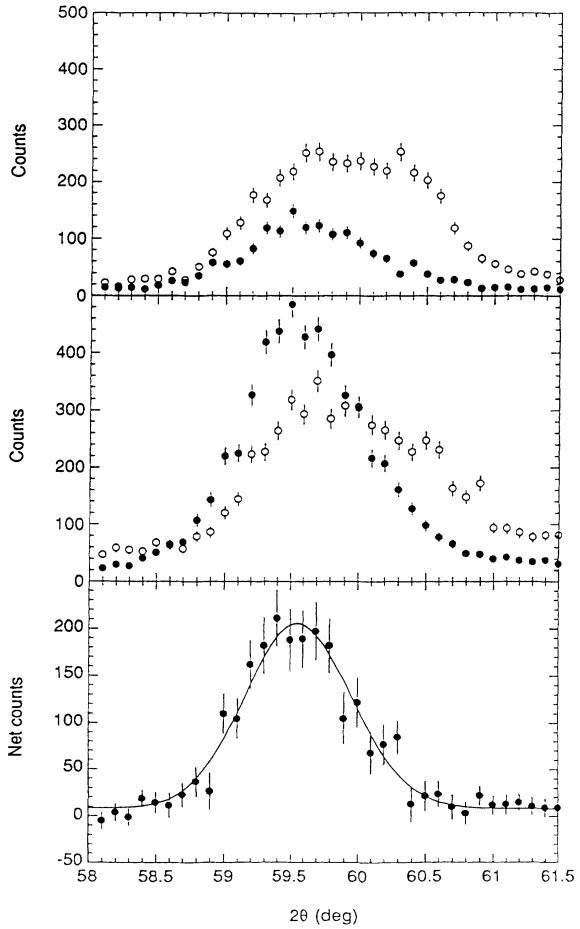

FIG. 3. Spin-flip (filled circles) and non-spin-flip (open circles) scattering for a peak at ~60°. The top portion is for $\mathbf{P}\perp\tau$, the center portion is for $\mathbf{P}\|\tau$, and the bottom portion is the subtraction of the spin-flip scattering for $\mathbf{P}\perp\tau$ from $\mathbf{P}\|\tau$.

of the 109 and 123 magnetic reflections at 59.36° and 59.66°, respectively (these reflections have indices $\frac{1}{2}\frac{1}{2}\frac{9}{2}$ and $\frac{3}{2}\frac{1}{2}\frac{3}{2}$ when referred to the cell of the nuclear structure).

All of the observed magnetic reflections have half-integral indices h,k,l when referred to the crystal axes of the nuclear structure and, consequently, all three axes of the magnetic unit cell are larger than those of the nuclear cell, as we have mentioned previously. This transformation can be due to a number of ordering arrangements of the magnetic moments, none of which can be excluded *a priori*. We have pointed out before, however, that the magnetic intensities present in the powder pattern of $YBa_2Fe_3O_8$ strongly suggest that the most probable model for the magnetic structure of the iron compound is one in which both the iron ions within the same layers, and the iron-containing layers stacked along the c axis, are coupled antiferromagnetically.

A model similar to that discussed in Ref. 20 was therefore refined together with the nuclear structure of initial

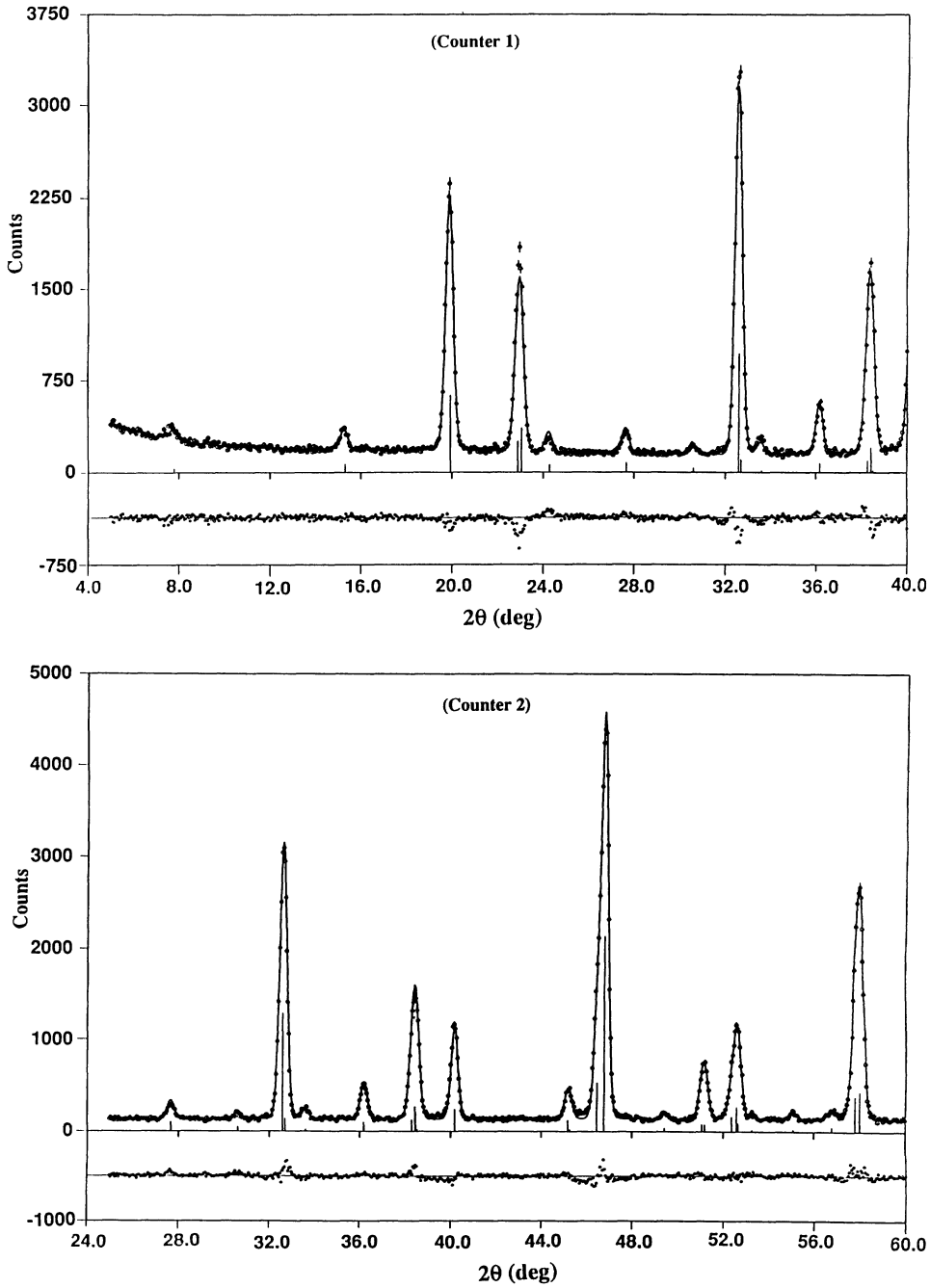

FIG. 4. Calculated (continuous line) and observed (circles) neutron profiles for each of the diffractometer's counters. The differences between calculated and observed intensities are plotted at the bottom of each figure.

parameters equal to those determined previously from the high-angle data. The magnetic form factor of iron used in these calculations was that calculated by Wood and Pratt.[21] This refinement gave very satisfactory agreement between observed and calculated intensities. Table II lists the results of the final refinement in which all nuclear and magnetic parameters were varied simultaneously, and Fig. 4 shows the experimental and calculated profiles for the five counters of the diffractometer. Relevant bond distances and angles are shown in Fig. 5. The magnetic moments refined to the same value for both Fe sites, within experimental error, and in the final refinement, we constrained them to be equal. The value obtained at room temperature for the ordered moment was $\langle \mu \rangle = 3.49(2)\mu_B$.

DISCUSSION OF THE NUCLEAR AND MAGNETIC STRUCTURES

The structure of $YBa_2Fe_3O_8$ is best discussed by comparing it to that of the original 1:2:3 superconductor. The atomic configurations of the two compounds may be described and compared to each other by representing them as sequences of layers in the following way:

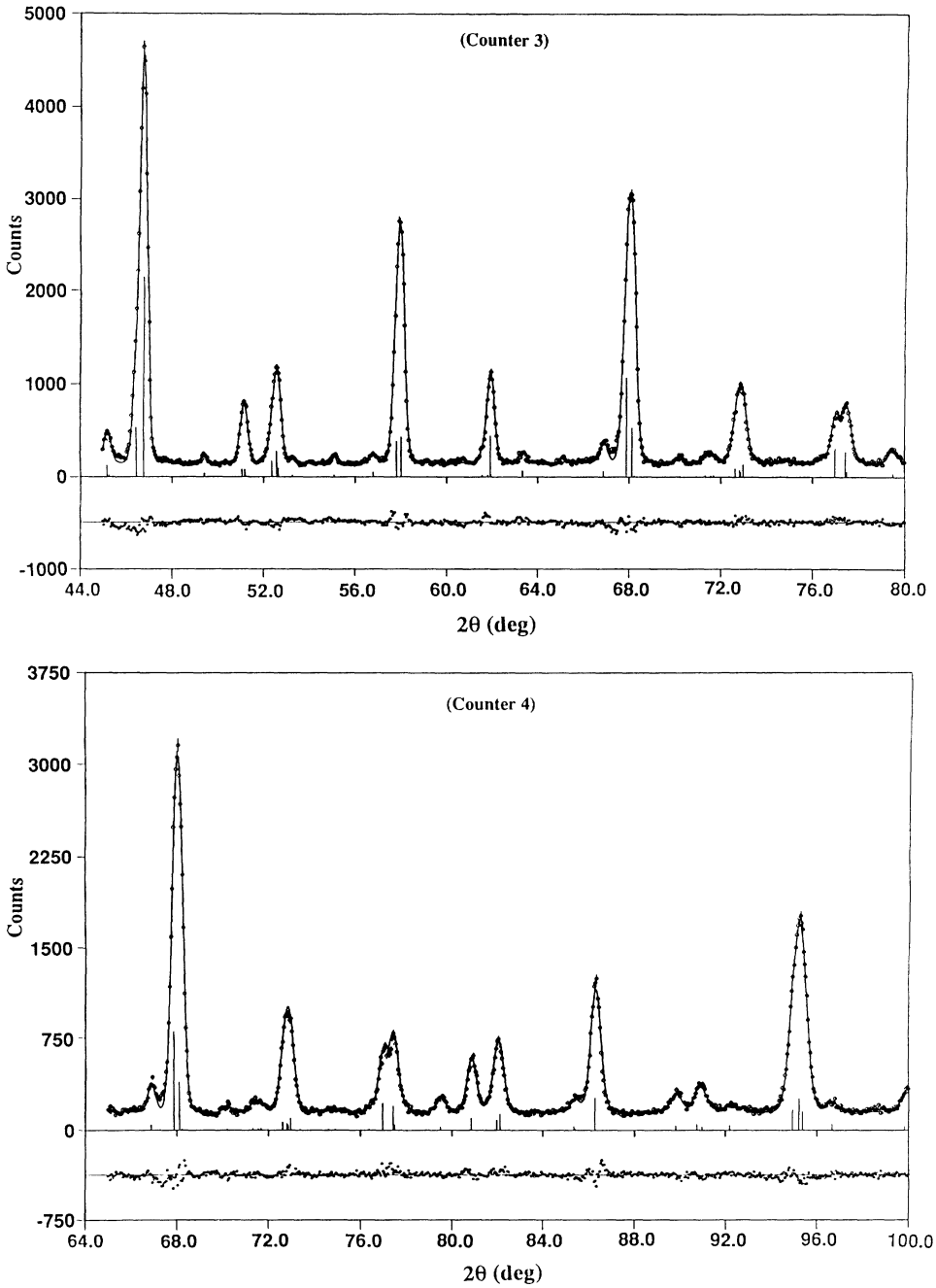

FIG. 4. (*Continued*).

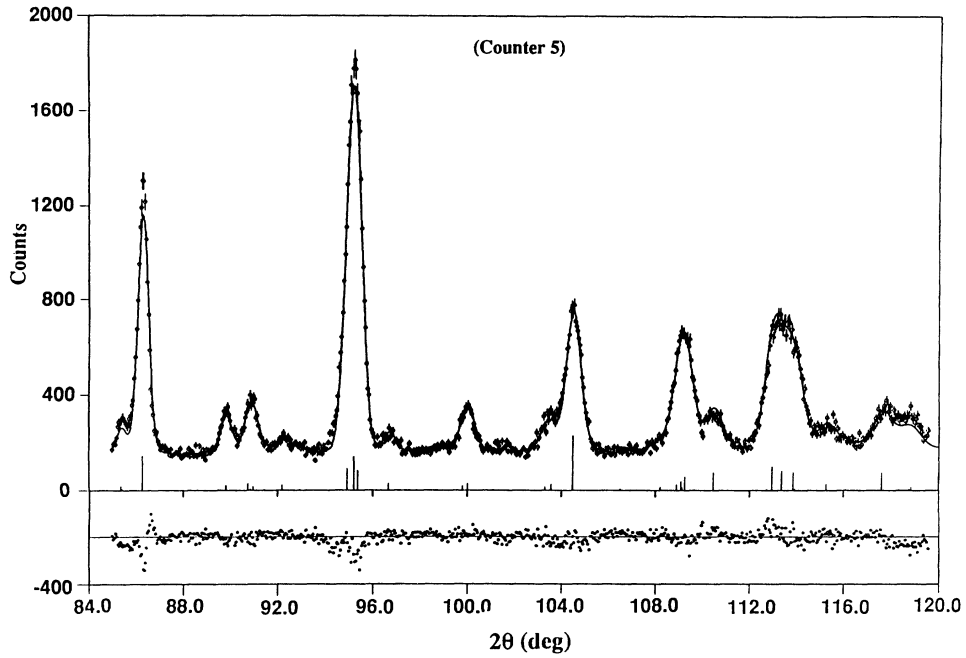

FIG. 4. (*Continued*).

$$\cdots[(FeO_2)_o(BaO)_c(FeO_2)_o(Y)_c(FeO_2)_o(BaO)_c](FeO_2)\cdots \quad YBa_2Fe_3O_8 ,$$

$$\cdots[(CuO_x)_o(BaO)_c(CuO_2)_o(Y)_c(CuO_2)_o(BaO)_c](CuO_x)\cdots \quad YBa_2Cu_3O_{6+x} .$$

In these formulas, the symbols in parentheses give the chemical composition of the layer, the subscripts o and c indicate if the cation is at the origin or at the center, respectively, of the layer's mesh, and the square brackets include the contents of one unit cell of the structure.[22] The sequence indicated in the above scheme for $YBa_2Fe_3O_8$ is also represented schematically in Fig. 6, where the structure of $YBa_2Fe_3O_8$ is compared with that of $YBa_2Cu_3O_{6+x}$ for $x=1$.

The main feature common to the two structures is the block of three layers $(FeO_2)_o(Y)_c(FeO_2)_o$ and $(CuO_2)_o(Y)_c(CuO_2)_o$. Because of this similarity, in both compounds the yttrium ions have eightfold prismatic coordination. The Y-O bond distances are also similar in

TABLE II. Refined structural parameters of $YBa_2Fe_3O_8$ at room temperature.

Chemical unit cell:
Space group: $P4/mmm$, $n=1$, $M_r=659.126$, $\rho_c=6.03$ g/cm^3
$a=3.9170(1)$, $c=11.8252(4)$ Å, $V=181.43(2)$ Å^3

Magnetic unit cell:
Orthorhombic, $a=5.5395(1)$, $b=5.5395(1)$, $c=23.6503(7)$ Å
$V=725.73(4)$ Å^3, $\mu_x=3.49(2)\mu_B$, $\mu_y=\mu_z=0$.

Atom	Position	x	y	z	B (Å^2)	Occupancy
Y	1*d* 4/*mmm*	$\frac{1}{2}$	$\frac{1}{2}$	$\frac{1}{2}$	0.76(7)	1
Ba	2*h* 4*mm*	$\frac{1}{2}$	$\frac{1}{2}$	0.1654(2)	0.78(2)	1
Fe(1)	1*a* 4/*mmm*	0	0	0	0.19(5)	1
Fe(2)	2*g* 4*mm*	0	0	0.3388(1)	0.79(5)	1
O(1)	2*g* 4*mm*	0	0	0.1804(2)	0.92(6)	1
O(2)	4*i* 2*mm*.	$\frac{1}{2}$	0	0.3783(1)	1.04(5)	1
O(3)	2*f* *mmm*.	0	$\frac{1}{2}$	0	1.04(8)	1

$R_{NM}=5.61$, $R_P=5.91$, $R_W=8.05$, $R_E=5.48$, $\chi=1.48$
$R_N=5.39$, $R_M=7.70$

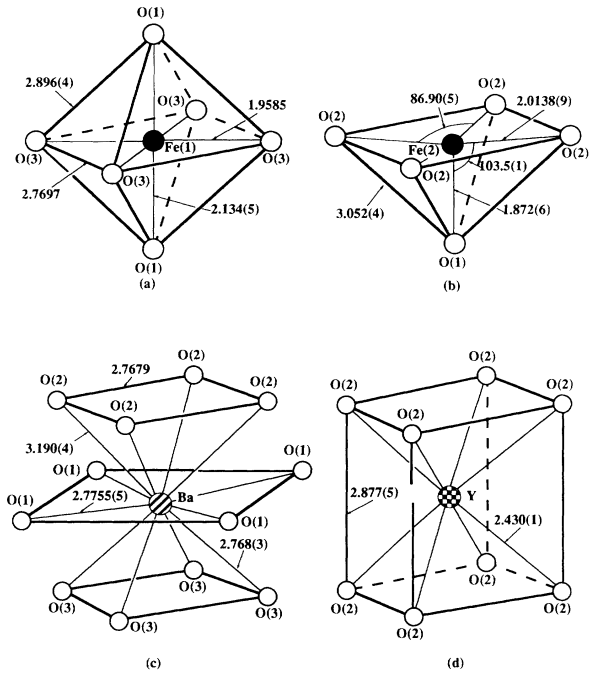

FIG. 5. Coordination polyhedra around (a) Fe(1); (b) Fe(2); (c) Ba; and (d) Y. The relevant bond distances and angles are indicated.

the two cases, with a value of 2.430 Å obtained in the present study and an average value of 2.398 Å in $YBa_2Cu_3O_7$.[23] The sequences $(BaO)_c(FeO_2)_o(Y)_c$ and $(Y)_c(FeO_2)_o(BaO)_c$ show that Fe(2) has fivefold pyramidal coordination analogous to that of Cu(2) in $YBa_2Cu_3O_{6+x}$, where the same sequences, with Cu instead of Fe, are also present. The Fe(2)-O distances in the pyramid range from 1.872 Å for the apical distance, to 2.014 Å for the in-plane separation (Fig. 5), with an average Fe(2)-O distance of 1.989 Å. These values are well within the limits found for the Fe-O separation in other compounds.

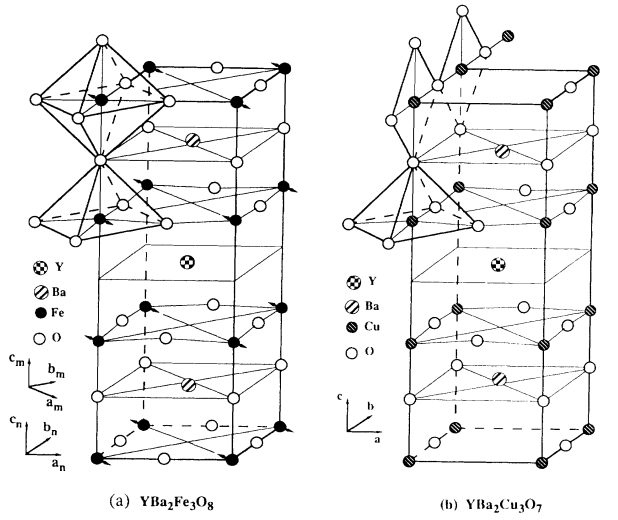

FIG. 6. (a) Nuclear and magnetic structures of $YBa_2Fe_3O_8$. For simplicity, only the nuclear cell is shown in the figure. The magnetic cell is related to the nuclear one by the transformation of axes matrix $(1\bar{1}0/110/002)$. The magnetic moments of the iron atoms lie in the planes perpendicular to c. Their direction in the plane, however, cannot be determined in our experiment and has been fixed arbitrarily along the a axis of the magnetic cell. (b) Unit cell of the compound $YBa_2Cu_3O_7$ shown for comparison with the iron compound.

The principal differences between the structures of $YBa_2Fe_3O_8$ and $YBa_2Cu_3O_{6+x}$ arise as a consequence of the different composition and atomic ordering of the layers of (CuO_x) and (FeO_2). Since $0 \leq x \leq 1$, the atoms Cu(1) have twofold linear coordination for $x=0$ and fourfold square-planar coordination for $x=1$, resulting in the well-known chain configuration along the b axis of the orthorhombic unit cell. The oxygen stoichiometry of $YBa_2Cu_3O_{6+x}$ affects also the coordination of the Ba atoms, which varies from eightfold to tenfold as the oxygen content increases from O_6 to O_7. On the other hand, the coordination polyhedra of Fe(1) are distorted octahedra with Fe(1)-O distances of 1.959 and 2.134 Å and with an average distance of 2.017 Å. These octahedra do not form chains but are arranged in a layer with the shared corners along the a and b directions of the unit cell. Because of the full occupancy of the oxygen sites on the $Fe(1)O_2$ layers above and below the plane of BaO, the coordination of Ba in the iron compound is twelvefold, as it would be in perovskite, and the coordination polyhedron of the Ba ions is a distorted cuboctahedron with Ba-O distances ranging from 2.768 to 3.190 Å.

The chemical and structural results obtained in this study give a composition corresponding to the formula $YBa_2Fe_3O_{8.00(3)}$. This indicates that the average oxidation number of the iron ions is +3. This average valence is distributed over two crystallographically inequivalent sites, Fe(1), with octahedral coordination, and Fe(2), with square-pyramidal coordination. The equal values of the magnetic moments of Fe(1) and Fe(2) obtained in the refinement of the magnetic structure, are a strong indication that the iron valence for the two sites is essentially the same. The fact that the average bond distance Fe(2)-O (1.986 Å) is slightly shorter than the average distance Fe(1)-O (2.017 Å) lends some support to this hypothesis. However, bond-length bond-strength calculations carried out using the formalism and the parameters discussed by Brown and Altermatt,[24] give +3.06 for the valence of Fe(1) and +2.75 for that of Fe(2). These numbers are approximate and do not provide convincing evidence for equal valence at the two iron sites. They show, however, that the two valences are not widely different from one another.

As we have mentioned previously, the magnetic structure represented in Fig. 6 is consistent with a unit cell related to the nuclear cell by the relations

$$\mathbf{a}_m = \mathbf{a}_n - \mathbf{b}_n \ , \quad \mathbf{b}_m = \mathbf{a}_n + \mathbf{b}_n \ , \quad \mathbf{c}_m = 2\mathbf{c}_n \ .$$

This transformation of axes gives a body-centered magnetic cell because the moduli of the magnetic moments are the same for all the iron atoms (as shown in Table II), and because the moments are arranged antiferromagneti-

cally both within the (FeO_2) planes and along the c axis. These structural features limit the indices of the allowed magnetic reflections to values with $l_M = 2n + 1$ (and, as a consequence, $h_M + k_M = 2n + 1$), i.e., to triplets with all indices fractional if the cell of the nuclear structure is used to describe the diffraction pattern. If we adopt the symmetry operations usually applied to magnetic structures,[25] the magnetic symmetry of $YBa_2Fe_3O_8$ becomes orthorhombic with space group $I_c mm'm$, where the primed symbol indicates that the secondary lattice direction is perpendicular to an antireflection operation.

A full knowledge of the magnetic behavior of the title compound can only be obtained by investigating the magnetic properties as functions of temperature. In particular, it will be interesting to ascertain if there are magnetic transitions involving rotations of the spin in the Fe(2) layers of the type discussed by Li, Lynn, and Fisk for $NdBa_2Cu_3O_{6+x}$.[20] Experiments at low and high temperature are now in progress and the results are planned to be published in due course.

[1]P. Bordet, J. L. Hodeau, P. Strobel, M. Marezio, and A. Santoro, Solid State Commun. **66**, 435 (1988).

[2]B. D. Dunlap, J. D. Jorgensen, C. Segre, A. E. Dwight, J. L. Matykiewicz, H. Lee, W. Peng, and C. W. Kimball, Physica C **158**, 397 (1988).

[3]G. Roth, H. Geger, B. Renker, J. Pannetier, V. Caignaert, M. Hervieu, and B. Raveau, Z. Phys. B **71**, 43 (1988).

[4]R. Sonntag, D. Hohlwein, A. Hoser, W. Prandl, W. Schaefer, R. Kiemel, S. Kemmler-Sack, S. Loesch, M. Schlichermeier, and A. W. Hewat, Physica C **159**, 141 (1989).

[5]M. Z. Cieplak, G. Xiao, C. L. Chien, J. K. Stalick, and J. J. Rhyne, Appl. Phys. Lett. **57**, 934 (1990).

[6]G. Xiao, M. Z. Cieplak, D. Musser, A. Gavrin, F. H. Streitz, C. L. Chien, J. J. Rhyne, and J. A. Gotaas, Nature **332**, 238 (1988).

[7]G. Roth, P. Adelmann, R. Ahrens, B. Blank, H. Buerkle, F. Gompf, G. Heger, M. Hervieu, M. Nindel, B. Obst, J. Pannetier, B. Raveau, B. Renker, H. Rietschel, B. Rudolph, and H. Wuehl, Physica C **162-164**, 518 (1989).

[8]M. Murayama, E. Sudo, K. Kani, A. Tsuzuki, S. Kawakami, M. Awano, and Y. Terii, Jpn. J. Appl. Phys. **27**(2), L1623 (1988).

[9]C. Greaves and P. R. Slater, Physica C **161**, 245 (1989).

[10]M. J. Rey, P. Dehaudt, J. Joubert, and A. W. Hewat, Physica C **167**, 162 (1990).

[11]G. Roth, P. Adelmann, G. Heger, R. Knitter, and T. Wolf, J. Phys. (Paris) **1**, 721 (1991).

[12]S. A. Sunshine, L. F. Schneemeyer, T. Siegrist, D. C. Douglass, J. V. Waszczak, R. J. Cava, E. M. Gyrogy, and D. W. Murphy, Chem. Mater. **1**, 331 (1989).

[13]Q. Huang, A. Santoro, and R. J. Cava (unpublished).

[14]S. Geremia, G. Nardin, R. Mosca, L. Randaccio, and E. Zangrando, Solid State Commun. **72**, 333 (1989).

[15]P. H. Andresen, H. Fjellvog, P. Karen, and A. Kjekshus, Acta Chem. Scand. (to be published).

[16]H. M. Rietveld, J. Appl. Crystallogr. **2**, 65 (1969).

[17]E.Prince, Nat. Bur. Stand. (U.S.) Tech. Note 1117, edited by F. J. Shorten, p. 8.

[18]R. M. Moon, T. Riste, and W. C. Koehler, Phys. Rev. **181**, 920 (1969).

[19]J. W. Lynn, W-H. Li, H. A. Mook, B. C. Sales, and Z. Fisk, Phys. Rev. Lett. **60**, 2781 (1988).

[20]W-H. Li, J. W. Lynn, and Z. Fisk, Phys. Rev. B **41**, 4098 (1990).

[21]J. H. Wood and G. W. Pratt, Phys. Rev. **107**, 995 (1957).

[22]A. Santoro, F. Beech, M. Marezio, and R. J. Cava, Physica C **156**, 693 (1988).

[23]S. Miraglia, F. Beech, A. Santoro, D. Tran Qui, S. A. Sunshine, and D. W. Murphy, Mater. Res. Bull. **22**, 1733 (1987).

[24]I. D. Brown and D. Altermatt, Acta Crystallogr. B **41**, 244 (1985).

[25]G. E. Bacon, *Neutron Diffraction*, 3rd ed. (Clarendon, Oxford, England, 1975), pp. 275ff.